ARTICLE

ACS chemical biology

Small Molecule Inhibitors of Yeast Pre-mRNA Splicing

Kelly G. Aukema[†], Kamalprit K. Chohan[†], Guy L. Plourde, Kerry B. Reimer, and Stephen D. Rader*

Department of Chemistry, University of Northern British Columbia, 3333 University Way, Prince George BC V2N 4Z9, Canada. [†]These authors contributed equally to this work.

ABSTRACT The spliceosome catalyzes pre-messenger RNA (pre-mRNA) splicing, an essential process in eukaryotic gene expression in which non-protein-coding sequences are removed from pre-mRNA. The spliceosome is a large, molecular complex composed of five small nuclear RNAs (snRNAs) and over 100 proteins. Large-scale rearrangements of the snRNAs and their associated proteins, including changes in base-pairing partners, are required to properly identify the intron-containing pre-mRNA, position it within the spliceosome, and complete the cleavage and ligation reactions of splicing. Despite detailed knowledge of the composition of the spliceosome at various stages of assembly, the critical signals and conformational changes that drive the dynamic rearrangements required for pre-mRNA splicing remain largely unknown. Just as ribosome-binding antibiotics facilitated mechanistic studies of the ribosome, study of the catalytic mechanisms of the spliceosome could be enhanced by the availability of small molecule inhibitors that block spliceosome assembly and splicing at defined stages. We sought to identify inhibitors of *Saccharomyces cerevisiae* splicing by screening for small molecules that block yeast splicing *in vitro*. We identified 10 small molecule inhibitors of yeast splicing, including four antibiotics, one kinase inhibitor, and five oxaspiro compounds. We also report that a subset of the oxaspiro derivatives permitted assembly of spliceosomal complexes onto pre-mRNA but blocked splicing prior to the first cleavage reaction.

The spliceosome catalyzes precursor-messenger RNA (pre-mRNA) splicing, the removal of non-protein-coding introns from pre-mRNA, which is an essential and tightly regulated step in eukaryotic gene expression. The boundaries between introns and protein-coding exons in pre-mRNAs are marked by consensus splice sites, which are recognized by components of the spliceosome to catalyze the two chemical steps of splicing, namely, reaction of the branch point adenosine with the 5′ splice site and subsequent ligation of the two exons with concomitant removal of the intron. The spliceosome assembles onto pre-mRNA primarily as small nuclear ribonucleoprotein (snRNP) particles, each consisting of a small nuclear RNA (snRNA) and its associated proteins (Figure 1). To identify and position the intron-delineating splice sites in the catalytic core of the spliceosome, large-scale rearrangements of the five snRNAs and over 100 proteins are required. As a result, the snRNA components of the spliceosome change secondary structure and base-pairing partners multiple times throughout the splicing cycle (*1*). The large size of the spliceosome, five MDa, and its highly dynamic reaction mechanism make it refractory to detailed structural and biochemical analysis. To determine how the core splicing machinery mediates splicing regulation, it is necessary to determine its structure at each step of the reaction pathway. Substantial progress has been made toward determining the composition and low-resolution structure of the spliceosome at various stages of assembly (*2*–*11*). However, numerous questions remain concerning the mechanism of catalysis and the regulation of spliceosome assembly. Elucidation of signaling mechanisms will be critical for understanding the regulation of the dynamic rearrangements that occur during splicing. Our ability to investigate these questions will be substantially enhanced by the availability of specific inhibi-

*Corresponding author, rader@unbc.ca.

Received for review April 15, 2009 and accepted July 27, 2009.

Published online July 28, 2009

10.1021/cb900090z CCC: $40.75

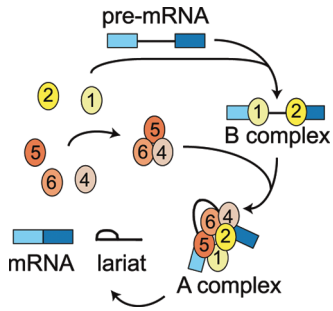

Figure 1. Model for spliceosome assembly onto pre-mRNA. U1 and U2 snRNP particles bind the 5′ splice site and the branch point, respectively, forming the B complex. Subsequent addition of the preformed triple snRNP (U4/U6, U5) results in the A complex. Within the A complex, the excised intron (lariat) and mature RNA splicing products are formed by two transesterification reactions in which the branch point adenosine attacks the 5′ splice site, allowing subsequent exon ligation as the freed 3′ hydroxyl of the 5′ exon attacks the 3′ splice site.

tors that block spliceosome assembly and splicing at defined stages.

Demonstrating their utility, small molecule inhibitors have underpinned dramatic advances in our understanding of protein translation over the past two decades. Antibiotics such as kirromycin and fusidic acid have been employed to trap the ribosome at specific steps with a sufficient degree of homogeneity to allow structure determination by NMR, X-ray crystallography, and cryo-electron microscopy (*12–15*). In addition, streptomycin and puromycin have provided insights into the translation mechanism by inhibiting the ribosome at specific points in its reaction cycle, producing stalled complexes that can then be studied by a variety of biochemical techniques (*16–18*). From these studies, we have gained a detailed understanding of the mechanisms of high-fidelity codon recognition and peptide bond formation (*19*). Likewise, it is expected that the study of the spliceosome will benefit greatly from the discovery of specific and effective inhibitors.

Previous studies have identified a diverse set of protein and small molecule inhibitors of mammalian splicing. The protein inhibitors of splicing range from domains of splicing proteins (CDC5L and PLRG1) and alternative splicing regulators (Fox-1/ Fox-2) to peptide inhibitors of CaMK-II-like protein and human protein phosphatase 1 (*20–24*). The small molecule inhibitors of mammalian splicing include antibiotics (erythromycin, Cl-tetracycline, and streptomycin) (*25*), a biflavonoid (isoginkgetin) (*26*), inhibitors of the kinase activity of topoisomerase I (*27, 28*), antitumor drugs targeting the U2 snRNP (Spliceostatin A and pladienolide) (*29, 30*), and inhibitors of histone deacetylases and histone acetyltransferases (*31*).

To date there are no published reports of small molecule inhibitors of *Saccharomyces cerevisiae* splicing, despite its recognition as a powerful system in which to study splicing. We therefore aimed to identify inhibitors by screening small molecules for their ability to inhibit yeast splicing *in vitro*. We report the identification of 10 yeast-splicing inhibitors, including four antibiotics, one kinase inhibitor, and five oxaspiro compounds. Two of the antibiotics uniquely inhibit *S. cerevisiae* splicing but not human splicing. We determine an apparent IC_{50} for each inhibitor and show that four of the oxaspiro derivatives allow substantial assembly of the pre-mRNA substrate into spliceosomal complexes but prevent the first cleavage reaction of splicing. We anticipate that these compounds will be useful for mechanistic studies of pre-mRNA splicing.

RESULTS AND DISCUSSION

To search for molecules that inhibit yeast pre-mRNA splicing at specific steps, we initially tested 26 compounds for their effects on splicing using an *in vitro* assay (Table 1). Eleven of the compounds tested were antibiotics chosen both to represent a range of antibiotic families and to allow comparison with inhibitors of human splicing (*25, 32*). Thirteen compounds were precursors of the manumycin family of antibiotics (*33*), chosen for the wide range of biological activities exhibited by the family, including antibacterial, insecticidal, tumoricidal, and anti-inflammatory (*34*). Finally, two kinase inhibitors were tested because protein phosphorylation is known to be important for human spliceosome assembly (*27, 28, 35*).

To measure the effect of the small molecules on splicing of yeast pre-mRNA, each compound was added to a standard yeast splicing reaction with actin pre-mRNA, and the efficiency of splicing was determined after 30 min. Whereas uninhibited splicing extracts support splicing of 40–55% of the actin *in vitro* transcript (Figure 2, lane 2), eight of the compounds tested reduced splicing to undetectable levels (Figure 2, lanes 4–11). The oxaspiro compounds and staurosporine were solubilized in DMSO. Because the addition of

TABLE 1. Candidate inhibitors of pre-mRNA splicing

Small molecule	Class	Splicing inhibition
Kanamycin	Aminoglycoside	Yes
Neomycin B	Aminoglycoside	Yes
Streptomycin	Aminoglycoside	Yes
Cefoperazone	Cephalosporin	Yes
Erythromycin	Macrolide	No[a]
Tetracycline	Aminocyclitol	No[a]
Ampicillin	Penicillin	No[a]
Ciprofloxacin	Quinolone	No[a]
Bacitracin	Polypeptide	No[a]
Sulfamethizole	Sulfonamide	No[a]
Chloramphenicol	Phenicol	No[a]
G5, G6, G11, G12 and G14	Oxaspiro	Yes[b]
G2–G4, G7–G10, G13	Phenolics	No[a,b]
Staurosporine	Broad range protein kinase inhibitor	Yes[b]
Roscovitine	Cyclin-dependent kinase inhibitor	No[c]

[a]Non-inhibitory at 10 mM. [b]Compounds tested in DMSO. [c]Non-inhibitory at 5.0 mM

DMSO consistently reduced uninhibited pre-mRNA splicing up to 40%, an additional control with DMSO (*i.e.*, no inhibitor) was included in each experiment (Figure 1, lane 3). Cefoperazone and staurosporine reduced splicing by approximately 50% and greater than 95%, respectively, at the maximum concentration testable due to solubility limitations (Figure 2, lanes 12 and 13). The remaining compounds had no effect on splicing efficiency (data not shown). To our knowledge, this is the first published report identifying small molecule inhibitors of *S. cerevisiae* splicing.

The splicing inhibitors clustered primarily in two classes: aminoglycoside antibiotics and oxaspiro derivatives (Table 1). All three aminoglycosides tested, kanamycin, streptomycin, and neomycin, inhibited splicing. Neomycin was the strongest inhibitor identified in this study, abolishing splicing at micromolar concentrations. Of the eight other classes of antibiotics tested, only cefoperazone, a cephalosporin, was inhibitory, suggesting that the majority of antibiotics do not negatively affect yeast splicing.

Aminoglycosides consist of sugar moieties decorated with positively charged amino groups, which facilitate binding to RNA through interactions with the negatively charged phosphate backbone. Aminoglycosides have been shown to inhibit both the ribosome and ribozymes through direct interaction with RNA (*36–38*). Therefore, it is reasonable to hypothesize that aminoglycosides interact directly with an snRNA component of the spliceosome or with the pre-mRNA substrate to block splicing.

The second class of small molecules found to inhibit yeast splicing is the oxaspiro compounds, G5, G6, G11, G12, and G14 (*33, 39, 40*), all of which are potential intermediates in syntheses of manumycin analogs. While manumycin A is a farnesyltransferase inhibitor (*41*), it has also been found to inhibit I κB kinase activity by a mechanism independent of farnesyltransferase inhibition (*42*). These studies suggest that manumycin analogues exert their inhibitory effects by interacting with specific protein enzymes. Therefore, spliceosomal proteins are potential targets of the oxaspiro derivatives tested.

We tested two protein kinase inhibitors to determine if they inhibit splicing. Mammalian splicing has long been known to involve a cycle of phosphorylation and dephosphorylation (*21*), and recently, in *S. cerevisiae* a comparison of transcript-specific splicing under various environmental stress conditions provided evidence of signal-regulated splicing as well (*43*). In yeast extract, splicing inhibition was detectable in the presence of the broad range protein kinase C inhibitor, staurosporine,

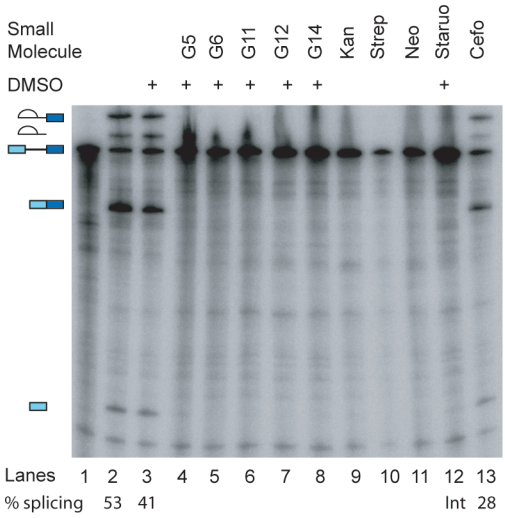

Figure 2. Splicing inhibition by 10 small molecules. ^{32}P-labeled actin pre-mRNA splicing reactions were analyzed on a 6% denaturing polyacrylamide gel and visualized by autoradiography. The mobility of splicing products and intermediates are indicated at left, from top to bottom: lariat-exon2, lariat, pre-mRNA, mRNA, and exon1. Splicing proceeded for 0 min (lane 1) or 30 min (lanes 2–13). Reactions were carried out in the absence (lanes 1–3) or presence (lanes 4–13) of small molecule in the following order: G5 (10 mM), G6 (5 mM), G11 (10 mM), G12 (5 mM), G14 (30 mM), kanamycin (5 mM), streptomycin (10 mM), neomycin (0.5 mM), staurosporine (3 mM), or cefoperazone (10 mM). Reactions containing 10% DMSO are marked (+). Splicing efficiency is indicated below each lane where splicing is detectable. Splicing intermediates (Int) are detectable in the presence of staurosporine (lane 12).

but not the high specificity cyclin-dependent kinase (CDK) inhibitor, roscovitine (Figure 2 and Table 1). The observed inhibition of yeast splicing by staurosporine raises the possibility that signaling kinases are involved, which is consistent with the observation that environmental conditions influence splicing in a transcript-specific manner in yeast (*43*). However, because staurosporine is a potent but non-specific inhibitor of kinases through interactions with the ATP binding pocket (*44*), it is also possible that staurosporine exerts its inhibitory effect on yeast splicing by blocking ATP binding to any of the DEXD/H-box RNA helicases involved in splicing. The lack of splicing inhibition in the presence of roscovitine suggests that cyclin-dependent kinases may not be involved in yeast splicing, but this possibility cannot be excluded, as roscovitine may not inhibit yeast CDKs.

The small molecule inhibitors, especially those known to bind RNA, may exert their effect on yeast splicing by interacting with the pre-mRNA. To test whether the inhibitory activity of these compounds is specific for actin pre-mRNA, the splicing assays were repeated with two other yeast transcripts, YOL047c and UBC4. The small molecules that completely inhibit actin splicing similarly reduced splicing of YOL047c and UBC4 to undetectable levels (data not shown), demonstrating that the observed inhibition is not transcript specific.

IC_{50} Determination. To determine the potency of our inhibitory compounds and to allow comparison to other reported splicing inhibitors, we measured the inhibitor concentration required for a 50% reduction in pre-mRNA splicing relative to a noninhibited control (apparent IC_{50}). Figure 3 shows the IC_{50} determination for the oxaspiro compound G5. At 6 mM G5, there is no detectable accumulation of splicing intermediates or spliced product, whereas at 0.1 mM, splicing efficiency is comparable to the uninhibited controls. Similar titration analysis was performed in triplicate for all inhibitory compounds. The IC_{50} values of these splicing inhibitors ranged from 80 μM for neomycin to 3 mM for G14 (Table 2), with the majority falling between 0.5 and 2 mM.

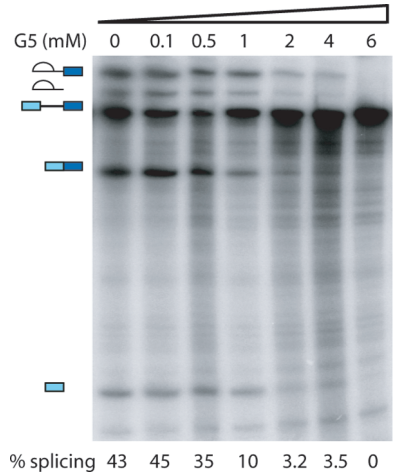

Figure 3. G5 inhibits pre-mRNA splicing with an apparent IC_{50} of 0.8 ± 0.2 mM. Denaturing polyacrylamide gel analysis of splicing with increasing concentration of G5, as indicated above gel. Locations of spliced products are indicated at left as in Figure 1, and the splicing efficiency is indicated below each lane.

TABLE 2. IC_{50} values of inhibitors

Inhibitor	IC_{50} (mM)[a]
Neomycin	0.08 ± 0.02
Kanamycin	0.4 ± 0.3
Streptomycin	1.0 ± 0.5
G5	0.8 ± 0.2
G6	0.6 ± 0.2
G11	1.7 ± 0.6
G12	0.7 ± 0.1
G14	3.0 ± 0.1
Staurosporine	1.8 ± 0.4

[a]Apparent IC_{50} values are the average of three measurements ± SD.

We compared inhibitory concentrations of the antibiotics assayed in yeast and human (HeLa) splicing systems. While inhibition of human splicing was observed at 500 μM erythromycin (*25*), no inhibition of yeast splicing by erythromycin was detectable up to 10 mM, suggesting that antibiotics may be useful for distinguishing mechanistic differences between yeast and human splicing. Of greater interest may be neomycin and kanamycin, as they inhibit yeast but not human splicing at similar concentrations. Neomycin and kanamycin inhibit yeast splicing with IC_{50} values of 80 and 400 μM, respectively, but neither was inhibitory for human splicing at 100 and 450 μM (*25, 32*). This differential effect of three antibiotics raises the intriguing possibility that identification of yeast-specific splicing inhibitors may prove to have therapeutic use as antifungal agents, as splicing is an essential process in pathogenic yeasts.

Inhibitor Effect on Spliceosomal Assembly. The discovery of a yeast splicing inhibitor with a specific block during spliceosome assembly would have important practical benefits for the study of the spliceosome. To determine the step of the splicing reaction at which our inhibitors exert their effects, we performed non-denaturing gel analysis on inhibited splicing reactions, monitoring the mobility of internally ^{32}P-labeled actin transcript as in standard splicing assays (Figure 4). The actin pre-mRNA, mRNA and two main spliceosomal assembly complexes can be distinguished on non-denaturing acrylamide gels in the presence of heparin to reduce non-specific binding. The faster mobility complex B is a precatalytic spliceosome containing U1 and U2 snRNP (see Figure 1) (*45*). The slower mobility complex A corresponds to the addition of U4, U5, and U6 triple snRNP to the pre-mRNA and likely contains multiple forms of the spliceosome, as a number of rearrangements are required to form the active spliceosome (*45*).

For an uninhibited reaction, the kinetics of appearance and disappearance of each assembly intermediate are similar to what has been reported previously (*45, 46*). The assembly pattern consists of a rapid decrease in pre-mRNA up to 5 min with a concomitant formation of the B complex, which is detected after 1 min and peaks between 2 and 15 min (Figure 4, panel a). Finally, the A complex is first detectable between one and five minutes, and remains at high levels throughout the remainder of the time course (Figure 4, panel a). Mature mRNA begins to accumulate at fifteen minutes.

Spliceosomal complex assembly was assayed in the presence of the inhibitors that completely blocked splicing, the antibiotic and oxaspiro compounds. Using the lowest inhibitor concentration tested that resulted in complete inhibition of splicing, the spliceosomal assembly pattern was analyzed by non-denaturing acrylamide gel electrophoresis after a standard splicing reaction (Figure 4, panel b). A fraction of each splicing reaction was simultaneously analyzed by denaturing gel electrophoresis to confirm complete splicing inhibition by each small molecule.

Splicing inhibitors can be categorized by which assembly intermediates accumulate in their presence (Figure 4). The principal species that accumulate for each inhibitor are listed in Table 3. The aminoglycosides (neomycin, kanamycin, and streptomycin) and the G12 oxaspiro compound prevented formation of spliceosomal complexes A and B. Four oxaspiro compounds, G5, G6, G11, and G14, allowed detectable accumulation of the A and B complexes. The portion of actin assembled into spliceosomal complexes was in the range of 10–20% of the total signal in the presence of G6, G11, and G14 and was as high as 45% in the presence of G5. With G5, we observe accumulation of similar amounts of A and B complexes, whereas with G6, G11, and G14 there is little or no A accumulation. Although there is detectable A complex in the presence of several of the oxaspiro compounds, no mature RNA or splicing intermediates are detectable by non-denaturing or denaturing gel electrophoresis (Figure 2 and 4), indicating that splicing has been blocked before

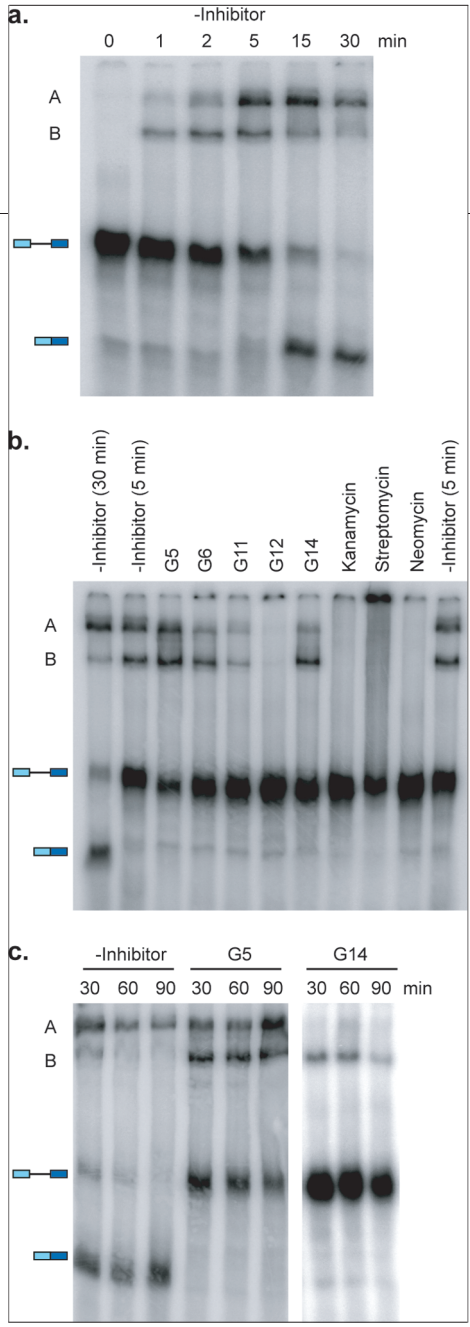

Figure 4. Splicing inhibitors stably block spliceosome assembly at distinct steps. a) Spliceosome assembly in the absence of small molecule monitored by non-denaturing acrylamide gel. The mobility of pre-mRNA, mRNA, and complexes A and B are indicated. Reaction times are indicated above each lane. b,c) Effect of splicing inhibitors on spliceosome assembly monitored by non-denaturing acrylamide gel. Inhibitor concentrations are listed in Figure 2. Complexes are labeled as in panel a. Assembly reactions proceeded for 30 min unless otherwise indicated above each lane.

the first chemical reaction that produces the lariat splicing intermediate and free exon.

The utility of the oxaspiro compounds as biochemical tools for splicing investigations depends greatly on the stability of the splicing complexes accumulated. To determine complex stability we assayed spliceosome assembly up to 90 min in the presence of G5, G14, G6, and G11 (Figure 4, panel c and data not shown). The levels of accumulated A and B complexes remained constant over 30–90 min in the presence of G14, G6, and G11, while the A complex continued to accumulate at 90 min in the presence of G5. Importantly, no detectable mature product formed in the presence of the inhibitors. We further confirmed inhibition of the chemical steps of splicing in the presence of G5 up to 2.5 h, as no splicing intermediates or products were detectable by denaturing gel electrophoresis (data not shown).

The oxaspiro derivatives G5, G6, G11, and G14 are the first identified small molecule inhibitors of yeast splicing that allow detectable accumulation of assembled complexes. Since the nature of the accumulated assembly intermediates is specific to the oxaspiro derivative added and the accumulated complexes are stable, these molecules may be useful tools for studying the biochemistry of spliceosome assembly. In particular, because the G6 and G14 compounds result in a strong, stable splicing block at the B complex, these compounds may provide the means to investigate the regulatory mechanisms responsible for triggering the addition of the triple snRNP (U4, U5, and U6 snRNA-containing species) to the pre-mRNA after the U1 and U2 snRNPs bind the 5′ splice site and branch point, respectively. Likewise, stable accumulation of the A complex in the presence of G5 may provide insights into the transitions required within the fully assembled spliceosome to catalyze the first chemical reaction of splicing.

Structural Features of Inhibitory Compounds. All of the inhibitory compounds identified in this study that allow some degree of spliceosome assembly are potential precursors in syntheses of manumycin analogs. The compounds tested in this study are either in an oxaspiro form with a second spirolactone ring or in the open, carboxylated form (Figure 5). Strikingly, we found that all of the compounds with a spirolactone ring inhibit splicing, while the nonoxaspiro compounds do not (Figure 5, panels a and b, respectively), indicating a high degree of specificity with respect to structure. These results suggest that the structural constraint conferred by the second ring is required for the inhibitory effect of these small molecules. These oxaspiro compounds have not been tested previously in any biochemical assay, so their activity as splicing inhibitors suggests this core structure may be a useful starting point for the design of compounds that are biologically active in a variety of contexts.

To test the hypothesis that a constrained second ring, rather than a lactone, *per se*, is a requirement for

TABLE 3. Assembly defects caused by inhibitors

Inhibitor	Accumulating assembly complexes
G5	A, B
G6	B, minor A
G11	B, minor A
G12	nd[a]
G14	B, minor A
Neomycin	nd[a]
Kanamycin	nd[a]
Streptomycin	nd[a]

[a]None detected

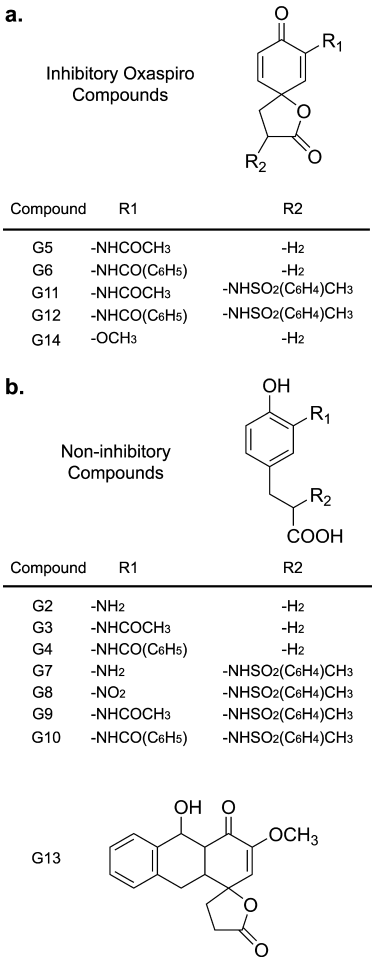

Figure 5. Oxaspiro-compound inhibitors share a common structure. a) Inhibitory oxaspiro derivates. b) Non-inhibitory compounds. The identity of the R1 and R2 groups is indicated.

splicing inhibition, we tested a compound with a spiroether second ring, G15 (Figure 6, panel b) (*47*), instead of a spirolactone second ring, as in G14 (Figure 5, panel a). Addition of G14 at 10 mM resulted in a reduction of splicing efficiency of 80%, while the same concentration of G15 resulted in a 17–35% reduction (Figure 6, panel a), suggesting that a spirolactone structure is important but not essential for efficient splicing inhibition. To further examine the importance of the carbonyl group in the spirolactone ring, we determined splicing efficiency in the presence of two oxaspiro derivatives in which the carbonyl group of the spirolactone is replaced with either an isopropyl or a *tert*-butyl alkyl group (Figure 6, panel b, G32 and G44) (*48–50*). While both of these compounds exhibited detectable splicing inhibition at 10 mM, reducing splicing by 20–40%, the superior inhibition by G14 again suggests that a spirolactone ring is an important feature of the inhibitory oxaspiro compounds.

To explore the important inhibitory features of the six-membered ring, we assayed splicing inhibition of an oxaspiro compound, G16 (*47*), with H_2 as the R1 group (Figure 6, panel b). We found that 10 mM G16 reduces splicing by approximately 50% and therefore does not inhibit splicing as well as G14 (Figure 6, panel a). Taken together with the apparent IC_{50} values determined for G5, G6, and G14 (Table 2), these data suggest that

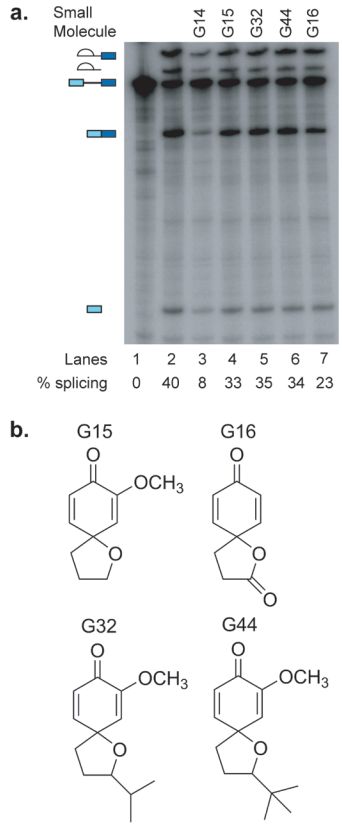

Figure 6. Oxaspiroether inhibition of splicing. a) Oxaspiroethers, G15, G32, G44, and spirolactone, G16, partially inhibit RNA splicing. Splicing proceeded for 0 min (lane 1) or 30 min (lanes 2–7). Reactions contained no small molecule (lanes 1 and 2) or the oxaspiro compounds indicated above each lane at 10 mM (lanes 3–7). The splicing efficiency is indicated below each lane. b) Structures of G15, G16, G32, and G44

larger R1 groups improve splicing inhibition of the spirolactone compounds. Future studies will focus on making modifications that will allow addition of a purification tag or a cross-linking moiety to the spirolactone compounds. These will be important both for determining the splicing target(s) of oxaspiro derivatives and for purification of stalled splicing complexes for biochemical characterization.

The identification of small molecules that inhibit yeast splicing is an important first step toward the ability to perform detailed biochemical studies of the yeast spliceosome. In addition to three aminoglycoside antibiotics and staurosporine, a broad range kinase inhibitor, we report on five oxaspiro compounds that inhibit yeast splicing with a high degree of specificity as structurally related phenolic compounds are not inhibitory. The ability to block splicing at a specific step during spliceosome assembly is a prerequisite for capture and release studies, such as those performed in the presence of acetyl transferase inhibitors (*31*), which will be necessary to determine the signals responsible for proceeding through specific steps within the splicing cycle. Four of the oxaspiro compounds that inhibit yeast splicing resulted in accumulation of intermediate splicing complexes during spliceosome assembly. These small molecule inhibitors may allow mechanistic insights into the spliceosome in a manner similar to what amnioglycosides have enabled for the ribosome.

METHODS

Small Molecules. Table 1 lists the initial compounds tested in this work. Antibiotics and kinase inhibitors were purchased from Sigma, and G compounds were synthesized according to published protocols (racemic mixtures, except G11 and G12) (*33, 39, 40, 47–52*). IUPAC chemical names for each G compound are provided in Supplementary Table 1.

Pre-mRNA Splicing Reactions. Whole-cell extract was prepared from protease deficient yeast strain BJ2168 as described (*53*). Pre-mRNA substrates for *in vitro* splicing assays were transcribed from 500 ng of linearized plasmid template (or 100 ng PCR-generated template) with T7 RNA polymerase (Roche) in the presence of 10 units of SUPERaseIN ribonuclease inhibitor (Applied Biosystems) and α^{32}P-GTP. Template for truncated ACT1 (actin, 590 nucleotides) was generated by linearizing BJPS149 plasmid with *Hin*dIII (*54, 55*). Templates for *in vitro* transcription of YOL047C (163 nucleotides) and UBC4 (290 nucleotides) were amplified by PCR from yeast genomic DNA (primers listed in Supplementary Table 2). The majority of unincorporated nucleotides were removed by centrifugation through a microspin G50 column according to manufacturer instructions (GE Healthcare).

Standard splicing of the actin pre-mRNA in BJ2168 nuclear extract was performed at 19 °C for 30 min. Splicing reactions were performed in 10-μL reactions containing 2.5 mM $MgCl_2$, 60 mM KPO_4 (pH 7.0), 3% PEG 3000, 40% (v/v) BJ2168 extract, 2 mM ATP, and 4 fmol of internally ^{32}P-GTP-labeled pre-mRNA *in vitro* transcript (*56*). Small molecule inhibitors were added to the splicing mix in 1 μL less than 5 min prior to addition of the pre-mRNA.

Denaturing Gels. Splicing reactions to be separated by denaturing gels were stopped by the addition of 200 μL of stop buffer (0.3 M Na acetate, 1 mM EDTA, 0.1% SDS, 34 mg mL^{-1} *E. coli* tRNA). The reactions were phenol/chloroform-extracted, ethanol-precipitated, and electrophoresed on a 6% denaturing, 7 M urea, polyacrylamide gel at 400 V for 1 h (Actin) or 35 min (YOL047C and UBC4). RNA bands were visualized and quantified with a Cyclone phosphorimager and Optiquant software (Packard Instruments). Splicing efficiency was defined as the percent of final product bands (mRNA and lariat) divided by the sum of all five bands (pre-mRNA, lariat-3′exon, 5′exon, excised lariat, and ligated exons). Splicing efficiencies were determined in triplicate.

IC_{50} Calculations. To calculate apparent IC_{50} values, each compound was titrated in the standard splicing reaction in triplicate and assayed by denaturing gel electrophoresis. Percent splicing was quantified for each compound concentration, normalized to the maximum percent splicing (an uninhibited reaction) and plotted versus inhibitor concentration. For each inhibitor, a line or curve fit to the data was used to determine the small molecule concentration that gives 50% splicing inhibition. The IC_{50} values were calculated as an average of three values with standard deviation as the error.

Spliceosomal Complex Assembly Gels. Aliquots of standard splicing reactions containing ^{32}P-labeled transcript were taken at the indicated times and adjusted to 0.7 mg mL^{-1} heparin and 12% glycerol with a trace of bromophenol blue. To separate individual spliceosomal complexes, samples were run on nondenaturing 4% polyacrylamide gels (80:1 acrylamide/bisacrylamide) at 160 V for 3 h in TGM buffer (50 mM tris base, 50 mM glycine, 2 mM $MgCl_2$). To confirm complete inhibition by small molecules of the splicing reactions analyzed by nondenaturing gel electrophoresis, an aliquot of each splicing reaction was also analyzed by denaturing gel. Gels were exposed to a phosphorimager screen for visualization.

Supporting Information Available: This material is available free of charge *via* the Internet at http://pubs.acs.org.

Acknowledgment: We thank T. Scully and R. Spaetzel for synthesizing compounds used in this study. We thank U. Kothe, A. Gorrell, M. Stark, and other members of the Rader lab for helpful discussions and comments on the manuscript. We acknowledge M. Stark, R. Mayas, B. Schwer, and B. Aukema for technical advice. This work was supported by NSERC Discovery Grant 298521 to S.D.R., a UNBC Health Research Project Award to K.K.C. and K.G.A., and Michael Smith Foundation for Health Research and Canadian Hemophilia Society postdoctoral fellowships to K.G.A. Financial contribution from the University of Northern British Columbia to G.L.P. is also acknowledged. Helpful and supportive suggestions by the anonymous reviewers of this manuscript are also gratefully acknowledged.

REFERENCES

1. Jurica, M. S. (2008) Detailed close-ups and the big picture of spliceosomes, *Curr. Opin. Struct. Biol. 18*, 315–320.

2. Jurica, M. S., Licklider, L. J., Gygi, S. R., Grigorieff, N., and Moore, M. J. (2002) Purification and characterization of native spliceosomes suitable for three-dimensional structural analysis, *RNA 8*, 426–439.
3. Jurica, M. S., Sousa, D., Moore, M. J., and Grigorieff, N. (2004) Three-dimensional structure of C complex spliceosomes by electron microscopy, *Nat. Struct. Mol. Biol. 11*, 265–269.
4. Boehringer, D., Makarov, E. M., Sander, B., Makarova, O. V., Kastner, B., Luhrmann, R., and Stark, H. (2004) Three-dimensional structure of a pre-catalytic human spliceosomal complex B, *Nat. Struct. Mol. Biol. 11*, 463–468.
5. Spadaccini, R., Reidt, U., Dybkov, O., Will, C., Frank, R., Stier, G., Corsini, L., Wahl, M. C., Luhrmann, R., and Sattler, M. (2006) Biochemical and NMR analyses of an SF3b155-p14-U2AF-RNA interaction network involved in branch point definition during pre-mRNA splicing, *RNA 12*, 410–425.
6. Deckert, J., Hartmuth, K., Boehringer, D., Behzadnia, N., Will, C. L., Kastner, B., Stark, H., Urlaub, H., and Luhrmann, R. (2006) Protein composition and electron microscopy structure of affinity-purified human spliceosomal B complexes isolated under physiological conditions, *Mol. Cell. Biol. 26*, 5528–5543.
7. Sander, B., Golas, M. M., Makarov, E. M., Brahms, H., Kastner, B., Luhrmann, R., and Stark, H. (2006) Organization of core spliceosomal components U5 snRNA loop I and U4/U6 Di-snRNP within U4/U6.U5 Tri-snRNP as revealed by electron cryomicroscopy, *Mol. Cell 24*, 267–278.
8. Behzadnia, N., Golas, M. M., Hartmuth, K., Sander, B., Kastner, B., Deckert, J., Dube, P., Will, C. L., Urlaub, H., Stark, H., and Luhrmann, R. (2007) Composition and three-dimensional EM structure of double affinity-purified, human prespliceosomal A complexes, *EMBO J. 26*, 1737–1748.
9. Hacker, I., Sander, B., Golas, M. M., Wolf, E., Karagoz, E., Kastner, B., Stark, H., Fabrizio, P., and Luhrmann, R. (2008) Localization of Prp8, Brr2, Snu114 and U4/U6 proteins in the yeast tri-snRNP by electron microscopy, *Nat. Struct. Mol. Biol. 15*, 1206–1212.
10. Bessonov, S., Anokhina, M., Will, C. L., Urlaub, H., and Luhrmann, R. (2008) Isolation of an active step I spliceosome and composition of its RNP core, *Nature 452*, 846–850.
11. Pomeranz Krummel, D. A., Oubridge, C., Leung, A. K., Li, J., and Nagai, K. (2009) Crystal structure of human spliceosomal U1 snRNP at 5.5 A resolution, *Nature 458*, 475–480.
12. Fourmy, D., Recht, M. I., Blanchard, S. C., and Puglisi, J. D. (1996) Structure of the A site of *Escherichia coli* 16S ribosomal RNA complexed with an aminoglycoside antibiotic, *Science 274*, 1367–1371.
13. Carter, A. P., Clemons, W. M., Brodersen, D. E., Morgan-Warren, R. J., Wimberly, B. T., and Ramakrishnan, V. (2000) Functional insights from the structure of the 30S ribosomal subunit and its interactions with antibiotics, *Nature 407*, 340–348.
14. Stark, H., Rodnina, M. V., Wieden, H. J., Zemlin, F., Wintermeyer, W., and van Heel, M. (2002) Ribosome interactions of aminoacyl-tRNA and elongation factor Tu in the codon-recognition complex, *Nat. Struct. Biol. 9*, 849–854.
15. Valle, M., Zavialov, A., Sengupta, J., Rawat, U., Ehrenberg, M., and Frank, J. (2003) Locking and unlocking of ribosomal motions, *Cell 114*, 123–134.
16. Sharma, D., Southworth, D. R., and Green, R. (2004) EF-G-independent reactivity of a pre-translocation-state ribosome complex with the aminoacyl tRNA substrate puromycin supports an intermediate (hybrid) state of tRNA binding, *RNA 10*, 102–113.
17. Kaul, M., Barbieri, C. M., and Pilch, D. S. (2004) Fluorescence-based approach for detecting and characterizing antibiotic-induced conformational changes in ribosomal RNA: comparing aminoglycoside binding to prokaryotic and eukaryotic ribosomal RNA sequences, *J. Am. Chem. Soc. 126*, 3447–3453.
18. Brunelle, J. L., Youngman, E. M., Sharma, D., and Green, R. (2006) The interaction between C75 of tRNA and the A loop of the ribosome stimulates peptidyl transferase activity, *RNA 12*, 33–39.
19. Moore, P. B., and Steitz, T. A. (2005) The ribosome revealed, *Trends Biochem. Sci. 30*, 281–283.
20. Lu, Y., Qian, X. Y., and Krug, R. M. (1994) The influenza virus NS1 protein: a novel inhibitor of pre-mRNA splicing, *Genes Dev. 8*, 1817–1828.
21. Mermoud, J. E., Cohen, P. T., and Lamond, A. I. (1994) Regulation of mammalian spliceosome assembly by a protein phosphorylation mechanism, *EMBO J. 13*, 5679–5688.
22. Parker, A. R., and Steitz, J. A. (1997) Inhibition of mammalian spliceosome assembly and pre-mRNA splicing by peptide inhibitors of protein kinases, *RNA 3*, 1301–1312.
23. Ajuh, P., and Lamond, A. I. (2003) Identification of peptide inhibitors of pre-mRNA splicing derived from the essential interaction domains of CDC5L and PLRG1, *Nucleic Acids Res. 31*, 6104–6116.
24. Zhou, H. L., and Lou, H. (2008) Repression of prespliceosome complex formation at two distinct steps by Fox-1/Fox-2 proteins, *Mol. Cell. Biol. 28*, 5507–5516.
25. Hertweck, M., Hiller, R., and Mueller, M. W. (2002) Inhibition of nuclear pre-mRNA splicing by antibiotics *in vitro*, *Eur. J. Biochem. 269*, 175–183.
26. O'Brien, K., Matlin, A. J., Lowell, A. M., and Moore, M. J. (2008) The biflavonoid isoginkgetin is a general inhibitor of pre-mRNA splicing, *J. Biol. Chem. 283*, 33147–33154.
27. Pilch, B., Allemand, E., Facompre, M., Bailly, C., Riou, J. F., Soret, J., and Tazi, J. (2001) Specific inhibition of serine- and arginine-rich splicing factors phosphorylation, spliceosome assembly, and splicing by the antitumor drug NB-506, *Cancer Res. 61*, 6876–6884.
28. Tazi, J., Bakkour, N., Soret, J., Zekri, L., Hazra, B., Laine, W., Baldeyrou, B., Lansiaux, A., and Bailly, C. (2005) Selective inhibition of topoisomerase I and various steps of spliceosome assembly by diospyrin derivatives, *Mol. Pharmacol. 67*, 1186–1194.
29. Kaida, D., Motoyoshi, H., Tashiro, E., Nojima, T., Hagiwara, M., Ishigami, K., Watanabe, H., Kitahara, T., Yoshida, T., Nakajima, H., Tani, T., Horinouchi, S., and Yoshida, M. (2007) Spliceostatin A targets SF3b and inhibits both splicing and nuclear retention of pre-mRNA, *Nat. Chem. Biol. 3*, 576–583.
30. Kotake, Y., Sagane, K., Owa, T., Mimori-Kiyosue, Y., Shimizu, H., Uesugi, M., Ishihama, Y., Iwata, M., and Mizui, Y. (2007) Splicing factor SF3b as a target of the antitumor natural product pladienolide, *Nat. Chem. Biol. 3*, 570–575.
31. Kuhn, A. N., van Santen, M. A., Schwienhorst, A., Urlaub, H., and Luhrmann, R. (2009) Stalling of spliceosome assembly at distinct stages by small-molecule inhibitors of protein acetylation and deacetylation, *RNA 15*, 153–175.
32. Zapp, M. L., Stern, S., and Green, M. R. (1993) Small molecules that selectively block RNA binding of HIV-1 Rev protein inhibit Rev function and viral production, *Cell 74*, 969–978.
33. Plourde, G. L., Spaetzel, R. R., Kwasnitza, J. S., and Scully, T. W. (2007) Diastereoselective spiroannulation of phenolic substrates: advances towards the asymmetric formation of the manumycin m-C7N core skeleton, *Molecules 12*, 2215–2222.
34. Sattler, I., Thiericke, R., and Zeeck, A. (1998) The manumycin-group metabolites, *Nat. Prod. Rep. 15*, 221–240.
35. Mathew, R., Hartmuth, K., Mohlmann, S., Urlaub, H., Ficner, R., and Luhrmann, R. (2008) Phosphorylation of human PRP28 by SRPK2 is required for integration of the U4/U6-U5 tri-snRNP into the spliceosome, *Nat. Struct. Mol. Biol. 15*, 435–443.
36. Moazed, D., and Noller, H. F. (1987) Interaction of antibiotics with functional sites in 16S ribosomal RNA, *Nature 327*, 389–394.
37. Stage, T. K., Hertel, K. J., and Uhlenbeck, O. C. (1995) Inhibition of the hammerhead ribozyme by neomycin, *RNA 1*, 95–101.
38. Hermann, T., and Westhof, E. (1998) Aminoglycoside binding to the hammerhead ribozyme: a general model for the interaction of cationic antibiotics with RNA, *J. Mol. Biol. 276*, 903–912.

39. Nishiyama, A., Eto, H., Terada, Y., Iguchi, M., and Yamamura, S. (1983) Anodic oxidation of 4-hydroxycinnamic acids and related phenols, *Chem. Pharm. Bull. 31*, 2845–2852.
40. Plourde, G. L., and Spaetzel, R. R. (2009) Synthesis of *N*-(2,8-dioxo-1-oxaspiro[4.5]deca-6,9-dien-7-yl) acetamide and benzamide, *Molbank* M599.
41. Hara, M., and Han, M. (1995) Ras farnesyltransferase inhibitors suppress the phenotype resulting from an activated ras mutation in Caenorhabditis elegans, *Proc. Natl. Acad. Sci. U.S.A. 92*, 3333–3337.
42. Bernier, M., Kwon, Y. K., Pandey, S. K., Zhu, T. N., Zhao, R. J., Maciuk, A., He, H. J., Decabo, R., and Kole, S. (2006) Binding of manumycin A inhibits IκB kinase β activity, *J. Biol. Chem. 281*, 2551–2561.
43. Pleiss, J. A., Whitworth, G. B., Bergkessel, M., and Guthrie, C. (2007) Rapid, transcript-specific changes in splicing in response to environmental stress, *Mol. Cell 27*, 928–937.
44. Karaman, M. W., Herrgard, S., Treiber, D. K., Gallant, P., Atteridge, C. E., Campbell, B. T., Chan, K. W., Ciceri, P., Davis, M. I., Edeen, P. T., Faraoni, R., Floyd, M., Hunt, J. P., Lockhart, D. J., Milanov, Z. V., Morrison, M. J., Pallares, G., Patel, H. K., Pritchard, S., Wodicka, L. M., and Zarrinkar, P. P. (2008) A quantitative analysis of kinase inhibitor selectivity, *Nat. Biotechnol. 26*, 127–132.
45. Cheng, S. C., and Abelson, J. (1987) Spliceosome assembly in yeast, *Genes Dev. 1*, 1014–1027.
46. Pikielny, C. W., Rymond, B. C., and Rosbash, M. (1986) Electrophoresis of ribonucleoproteins reveals an ordered assembly pathway of yeast splicing complexes, *Nature 324*, 341–345.
47. Tamura, Y., Yakura, T., Haruta, J., and Kita, Y. (1987) Hypervalent iodine oxidation of *p*-alkoxyphenols and related compounds: a general route to *p*-benzoquinone monoacetals and spiro lactones, *J. Org. Chem. 52*, 3927–3930.
48. Plourde, G. L. (2002) Studies towards the diastereoselective spiroannulation of phenolic derivatives, *Tetrahedron Lett. 43*, 3597–3599.
49. Plourde, G. L. (2003) Synthesis of (±)-7-methoxy-2-isopropyl-1-oxaspiro[4,5]deca-6,9-diene-8-one, *Molbank* M319.
50. Plourde, G. L. (2003) Synthesis of (±)-2-tButyl-7-methoxy-1-oxaspiro[4,5]deca-6,9-diene-8-one, *Molbank* M322.
51. Plourde, G. L., R., P., and B, L. D. (1999) Synthesis and characterization of 1-hydroxy-2-methoxy-4-(3-propanoic acid)anthracene, *Synth. Commun. 29*, 2895–2901.
52. Plourde, G. L., Susag, L. M., and Dick, D. G. (2008) Determination of the absolute configurations of (+)-*N*-((3*S*)-3-{[(4-methylphenyl)sulfonyl]amino}-1-oxaspiro[4.5]deca-6,9-dien-2,8-dion-7-yl) acetamide and benzamide, *Molbank* M579.
53. Ansari, A., and Schwer, B. (1995) SLU7 and a novel activity, SSF1, act during the PRP16-dependent step of yeast pre-mRNA splicing, *EMBO J. 14*, 4001–4009.
54. Vijayraghavan, U., Parker, R., Tamm, J., Iimura, Y., Rossi, J., Abelson, J., and Guthrie, C. (1986) Mutations in conserved intron sequences affect multiple steps in the yeast splicing pathway, particularly assembly of the spliceosome, *EMBO J. 5*, 1683–1695.
55. Mayas, R. M., Maita, H., and Staley, J. P. (2006) Exon ligation is proofread by the DExD/H-box ATPase Prp22p, *Nat. Struct. Mol. Biol. 13*, 482–490.
56. Schwer, B., and Guthrie, C. (1991) PRP16 is an RNA-dependent ATPase that interacts transiently with the spliceosome, *Nature 349*, 494–499.